Identification of daughter minerals in fluid inclusions using scanning electron microscopy and energy dispersive analysis

ELIZABETH Y. ANTHONY

Department of Geosciences
University of Arizona
Tucson, Arizona 85721

T. JAMES REYNOLDS

Fluid Inc., P. O. 6873
Denver, Colorado 80206

AND RICHARD E. BEANE

AMAX Exploration, Inc.
10 E. Broadway, Ste. 400
Tucson, Arizona 85701

Abstract

Scanning electron microscopy combined with energy dispersive analysis provides a method for identification of daughter minerals in fluid inclusions. Previous studies using this method have not applied absorption and fluorescence corrections to the spectrum; thus stoichiometry of the minerals was not determined and ambiguities in characterization remain. We have found that, despite the irregular surface geometry of daughter minerals in the fluid inclusions, use of standard data reduction programs yields compositions which are sufficiently accurate to allow identification in many instances.

Inclusions in quartz associated with early potassic alteration from the Santa Rita porphyry copper deposit, New Mexico, were examined in this study. Standard fluid inclusion plates revealed the existence of a number of minerals in the inclusions which met the criteria for daughter rather than trapped minerals, viz. occurrence of the same minerals, and the same proportions of phases, in many inclusions. These daughter minerals and their average elemental ratios as determined in this study are: halite (Na = 1.00, Cl = 1.00), sylvite (K = 1.07, Cl = 1.00), chalcopyrite (Cu = 1.06, Fe = 1.07, S = 2.00), anhydrite (Ca = 1.07, S = 1.00), potassium feldspar (K = 0.87, Na = 0.16, Al = 1.00), phengitic muscovite (K = 1.00, Al = 2.66, Fe = 0.56), and iron-rich trioctahedral mica (K = 1.00, Al = 3.16, Fe = 1.83).

Introduction

Fluid inclusions in hydrothermal minerals often contain daughter minerals which precipitated during cooling from the high temperatures of fluid entrapment. Identification of these minerals usually depends upon externally observed properties such as solubility, magnetism, crystal morphology, and birefringence (Roedder, 1972). Recently, more elaborate techniques have been employed. These include the extraction and X-ray diffraction analysis of individual daughter minerals (Zolensky and Bodnar, 1982), Raman spectrometric analysis (Rosasco and Roed-

der, 1979), and the use of scanning electron microscopy (SEM) and qualitative energy dispersive analysis (EDA) (Metzger et al., 1977; Wilson et al., 1980; Le Bel, 1976; Kelly and Burgio, 1983).

The SEM/EDA (microprobe) technique yields information on the morphology of the crystal and the elements present. Although analysis can be done on extracted material (Roedder, 1972), a simpler approach which is used in most studies is to break samples of host mineral and study the exposed daughter minerals *in situ* on fracture surfaces.

Previous studies have used raw peak intensities alone

as a rough measure of the abundance of elements in the daughter minerals, without benefit of data reduction schemes for correction of absorption and fluorescence. Stoichiometry is not resolved, and ambiguities in identification persist. We have discovered that, despite some difficulties, standard data reduction programs work well enough to allow identification of many different kinds of daughter minerals, even to the point of determining the compositions of phases which exhibit solid solution.

Perhaps the greatest concern in attempting quantitative analysis of the daughter minerals is that of geometry: the daughter minerals are small (ca. 1 to 10 μm across), there are often many minerals within the cavity of the opened inclusion, and the analyzed surface of an individual crystal is usually not perpendicular to the incident beam. These analytical conditions increase the likelihood that backscattered primary electrons will excite radiation in the host material and other daughter minerals, as well as in instrument components. In addition, characteristic radiation emitted by the analyzed daughter mineral may cause secondary fluorescence of lighter elements in surrounding minerals.

The daughter minerals discussed in this paper were found in hydrothermal quartz from the Santa Rita porphyry copper deposit, New Mexico. Characterization of daughter minerals was undertaken as part of a broader study concerning geothermometry and ore genesis at the Santa Rita deposit (Reynolds, 1980, Reynolds and Beane, in prep.). Optical examination which accompanied the geothermometric work provided the means to distinguish between trapped minerals—that is, solid mineral inclusions—and true daughter minerals—minerals which precipitated from fluid within the inclusion after entrapment. Criteria for determining that a crystal is a daughter mineral include "constancy of occurrence, and of volume percent, of each daughter mineral in several or many inclusions." (Roedder, 1972, p. JJ24.)

These criteria were met for a number of minerals; of these some could be tentatively identified during the optical investigation. Those identified by their physical and optical properties were halite and sylvite, both of which are cubic and show the appropriate dissolution behavior; magnetite, which was magnetic; hematite, which occurred as hexagonal, red flakes; and chalcopyrite, which was opaque and had triangular faces typical of tetrahedral habit. These minerals were also analyzed during the microprobe study. In addition we found translucent minerals which met the criteria for being daughter products but could not be identified by their optical properties. Because the technique used to fracture the quartz host was too imprecise to allow previously selected inclusions to be opened, the equivalence between these unidentified daughter products and the minerals observed during the microprobe study—potassium feldspar, micas, and anhydrite—is tentatively made. The correlation is made plausible by the fact that these minerals were found repeatedly during the microprobe study. Additional tests, such as staining (Metzger et al.,

1977) and X-ray diffraction, could be made in order to further strengthen the correspondence.

Analytical procedure

Sample preparation

Fragments of quartz known to contain fluid inclusions having daughter minerals were broken using a small anvil and mounted according to standard SEM techniques.

We chose to carbon-coat the samples, although gold coating provides better resolution and is more frequently used in SEM studies. This choice was made because the detector has a resolution of approximately 0.150 keV and thus the $AuM\alpha$ peak (2.123 keV) from the coating and the $SK\alpha$ peak (2.307 keV) from the sulfide daughter minerals overlap substantially. This interference can be corrected for in the data reduction, but we found that the slight loss in resolution experienced when using carbon-coated samples was more than amply re-paid by the convenience of removing the interference.

Analysis

An ARL scanning electron microprobe equipped with a Si(Li) energy dispersive detector was used. Operating conditions were: 15 kV accelerating voltage, 150 mA emission current, 1 nA sample current (measured on benitoite), and a fully focused beam—less than a few μm in diameter. Counting time for elemental determinations depended on the size of the daughter crystal, but was generally about 200 seconds for major element determinations. The standards were a combination of native elements, oxides, silicates, and sulfides used routinely in the SEMQ Laboratory at the University of Arizona.

Samples were scanned using low magnification until an opened inclusion was located. A photograph of the inclusion was taken so that the morphologies of the crystals within it could be correlated with their chemical compositions and to assist in relocating the inclusion. Peak intensities were calculated using the curve-fitting program, SUPERML, which is supplied by Tracor Northern for the ARL microprobe. In the initial stages of the study, the raw peak intensities of the daughter minerals were compared to those obtained for reference samples of the minerals. We found that the peak intensities of daughter minerals correlated quite well with those of reference samples and that individual daughter minerals gave reproducible results. (See, for example, Fig. 1.) The program ZAF, also supplied by Tracor Northern, was used to apply corrections for fluorescence and absorption to those peak intensities which had proven reproducible. Only peaks considered to have originated solely in the analyzed daughter mineral were included in the program, e.g. sodium and chlorine but not silicon for halite, and potassium, sodium, and aluminum but not silicon for potassium feldspar.

The success of analysis depends upon the size and orientation of the daughter mineral. Often we were able to obtain reasonable analyses of minerals as small as a few μm across. Although the radiation intensity from the daughter mineral is much less than that from the surrounding quartz, the ratios of elements belonging to the daughter mineral are often diagnostic. The greatest difficulties were encountered in dealing with clusters of small minerals because it was difficult to determine what radiation was contributed by each mineral. For example, spectra showing iron, sodium, potassium, and chlorine peaks were in some instances derived cumulatively from a cluster of halite, sylvite, and iron oxide daughter minerals. Observation of the crystal morphology often helps to unravel complex spectra.
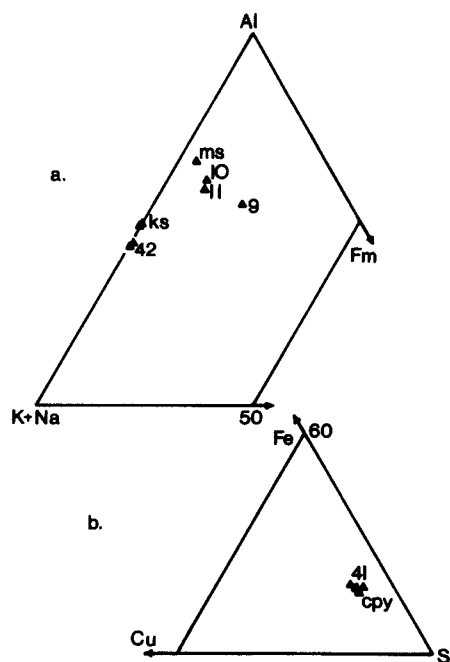
Fig. 1. Ternary diagrams of the *uncorrected* $K\alpha$ peak intensities for daughter minerals (numbered analyses) and reference materials (indicated by acronyms). Daughter mineral identification numbers correspond to those in Fig. 2 and Table 1. (a) ms = muscovite reference material, ks = potassium feldspar material. (b) cpy = chalcopyrite reference material.

Table 1. Representative analysis of daughter minerals and reference materials

HALITE - 3 ANALYSES OF DAUGHTER MINERAL J1

	WEIGHT PERCENT†				STOICHIOMETRY‡			
	1	2	3	std	1	2	3	std
Na	28.2	26.0	26.4	38.1	1.03	0.98	1.00	0.98
Cl*	42.3	40.9	40.9	60.2	1.00	1.00	1.00	1.00

CHALCOPYRITE - 3 ANALYSES OF DAUGHTER MINERAL 41

	WEIGHT PERCENT†				STOICHIOMETRY‡			
	1	2	3	std	1	2	3	std
Cu	27.1	29.0	25.9	33.9	1.05	1.07	1.05	0.98
Fe	24.3	25.3	25.0	30.5	1.08	1.06	1.06	1.01
S*	26.0	27.3	23.0	34.8	2.00	2.00	2.00	2.00

ANHYDRITE - 2 ANALYSES OF DAUGHTER MINERAL 13

	WEIGHT PERCENT†			STOICHIOMETRY‡		
	1	2	std	1	2	std
Ca	6.8	24.5	29.1	1.07	1.07	0.96
S*	5.0	18.1	24.3	1.00	1.00	1.00

POTASSIUM FELDSPAR - 2 ANALYSES OF DAUGHTER MINERAL 42

	WEIGHT PERCENT†			STOICHIOMETRY‡		
	1	2	std	1	2	std
K	10.0	9.7	12.5	0.95	0.87	0.89
Na	ni	1.1	1.5	ni	0.16	0.26
Al*	7.3	7.7	9.9	1.00	1.00	1.00

MICAS - DAUGHTER MINERALS 9 (trioct.); 10 and 11 (dioct.)

	WEIGHT PERCENT†					STOICHIOMETRY‡				
	9	10	11	std	std	9	10	11	std	std
K*	1.7	3.9	7.2	8.8	8.4	1.00	1.00	1.00	1.00	1.00
Fe	4.4	2.8	6.2	3.1	3.2	1.83	0.51	0.6	0.25	0.26
Al	3.6	7.6	12.4	16.2	18.4	3.16	2.82	2.49	2.58	3.16
Ti	nd	0.4	0.7	nd	nd	-	0.09	0.08	-	-
Si	ni	ni	ni	21.8	ni	-	-	-	3.34	-

†Weight percent does not include silicon from host material.
‡The atomic proportions, i.e., stoichiometries, are normalized to the element indicated by an asterisk.
The daughter mineral identification numbers correspond to those in Figs. 1 and 2. "Std" refers to reference materials analyzed using the same procedure as for daughter minerals.
nd = not detected, ni = not included in corrections program.

Salts deposited onto the surface of daughter minerals by evaporation when the inclusion is opened can also contribute spurious radiation to analyses, but the following evidence suggests that this material had a minimal effect in this study. First, there was no textural evidence such as splatter marks on the daughter minerals or the surrounding quartz. (For examples of visible coatings see Metzger et al., 1977, Fig. 5; Chryssoulis and Wilkinson, 1983; Kelly and Burgio, 1983.) Second, daughter minerals which were isolated contained only those elements intrinsic to the mineral plus silicon from the quartz host. We consider that complex spectra with subsidiary peaks seemingly unrelated to the analyzed mineral are caused predominantly by radiation from backscattered electrons and secondary fluorescence.

Other analytical difficulties include compositional totals which are substantially less than one hundred percent (Table 1). These low totals result from the exclusion of radiation belonging to the surrounding quartz and other daughter minerals from the corrections program. In addition, because absorption and fluorescence are matrix effects, the deletion of this spurious radiation from the corrections program introduces error in the relative amounts of the other elements. The magnitude of this error was evaluated by counting the peak intensities on standard silicate minerals and solving for the chemical composition both including the silicon intensities in the program and excluding them from the program. The maximum relative error, when silicon was included in the ZAF program, was typically less than five percent. The error increased to as much as ten percent when silicon was excluded from the program. An iterative approach, which would add the

requisite silicon after identification of the mineral, could well improve analytical results.

Results

Using the methods described above, a number of minerals were identified. They are discussed here by chemical type.

Chlorides

Halite and sylvite were found in abundance, and the analyses were adequate for characterization (Table 1, Fig. 2). Both of these are common daughter minerals in hypersaline fluid inclusions (Roedder, 1979).

The identification of potassium-iron chlorides, which have been suggested by others (Wilson et al., 1980; Le Bel, 1976) proved difficult. As discussed above, a number of analyses showed combinations of potassium, sodium, iron, and chlorine. Unfortunately, these crystals usually were very small, exhibited no crystal morphology within the limits of optical resolution, and occurred in clusters;
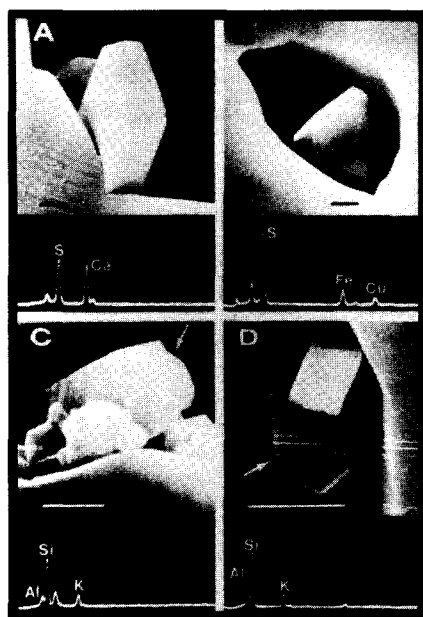
Fig. 2. Scanning electron microscope photographs, and corresponding energy dispersive spectra, of daughter minerals. Bar scale represents one micron. (a) orthorhombic anhydrite (?) (#13), (b) tetrahedral chalcopyrite, (c) monoclinic potassium feldspar (#42), and (d) pseudohexagonal dioctahedral mica, with a small iron oxide mineral (?) in the upper right.

thus it was not possible to isolate the radiation from individual minerals. To determine the magnitude of the interference, we analyzed a number of spots on individual minerals. Our assumption was that if the analyses were similar, extraneous radiation was minimal. Often these repetitive analyses differed radically. Further, the corrected peak intensities yielded stoichiometries which were not electrically balanced and did not resemble any known complex chloride mineral, viz. erythrosiderite ($K_2FeCl \cdot H_2O$) or rinneite ($K_3NaFeCl_6$). Generally, the amount of detected chloride was insufficient for the quantity of cations. It is possible that the minerals are compound hydroxide, carbonate, borate, or fluoride chlorides, such as the calcium fluoride chloride (CaFCl) reported by Kulikov et al. (1982). We could not assess this possibility because energy dispersive analysis is generally limited by the beryllium window to detection of elements with atomic number greater than neon.

Sulfides and sulfates

Pseudo-tetrahedra of chalcopyrite and a calcium sulfate with apparent orthorhombic habit were observed (Table 1, Fig. 1). The calcium sulfate is assumed from its morphology to be anhydrite, and this assumption is strengthened by the observation that one of the rectangular translucent minerals observed during the optical investigation showed parallel extinction. However, because water cannot be detected and cannot be calculated

by difference because of the low analytical totals, the energy dispersive analysis alone cannot resolve whether the analyzed crystals are gypsum or anhydrite.

The calcium sulfate analyses demonstrate an important finding of this work. The detected concentrations of calcium and sulfur differ considerably for the two analyses of the same daughter mineral (Table 1). The lower total results from the beam not sitting "squarely" on the crystal or hitting a face more inclined from the horizontal. However, after data reduction the ratios of calcium to sulfur are remarkably similar, and the stoichiometry, though limited to the cations, is reliable.

The occurrence of chalcopyrite as a daughter mineral is interesting because, for the samples studied, chalcopyrite *mineralization* was not associated with these high-salinity fluids but rather with low-salinity fluids (Reynolds, 1980; Reynolds and Beane, in prep.) Chalcopyrite daughter minerals in fluid inclusions in quartz not directly associated with copper mineralization have also been observed by Sawkins and Scherkenbach (1981).

Silicates

Potassium feldspar, muscovite, and a trioctahedral iron mica belonging to the siderophyllite-annite series were tentatively identified (Table 1, Fig. 1). The micas were recognized on the basis of their pseudohexagonal habit and the ratios of cations other than silicon. Dioctahedral muscovite may be written: $KAl_2(AlSi_3)O_{10}(OH)_2$. For this ideal mica, if formula units are normalized to potassium equal to one, the sum of tetrahedral plus octahedral aluminum is three. Deviation from this ratio occurs in phengitic muscovites, in which coupled substitution exists between ferrous iron in octahedral sites and silicon in tetrahedral sites. Thus the ratio of silicon to tetrahedral aluminum in phengitic muscovite is greater than 3:1 and the sum of tetrahedral aluminum plus octahedral cations decreases concomitantly.

Daughter minerals identified as dioctahedral micas have compositions for which the summation of iron, titanium, and aluminum is close to but greater than three (Table 1). Possible reasons for this excess include: (1) There may be a deficiency of potassium or substitution of H_3O^+ in the potassium site, such as occurs in hydromuscovite or illite. Because the sum of octahedral and tetrahedral cations was normalized to potassium equal to one, a value less than unity for potassium would cause a reduction in the sum. (Detected sodium or calcium in these minerals was negligible.) (2) Because silicon causes secondary fluorescence of aluminum, the deletion of silicon radiation from the correction program may result in inaccurately high aluminum values. Table 1 includes analyses of a nondaughter muscovite which show that the effect of deleting silicon from the ZAF program is to increase aluminum values from 16.2 to 18.4 weight percent while the values for other elements remain essentially constant.

A general formula for the trioctahedral micas is $K(Mg,Fe,Al)_3(Si,Al)_4O_{10}(OH)_2$. The sum of tetrahedral aluminum plus octahedral cations is four to five with potassium equal to one. The analysis included in Table 1 is magnesium-free and close to the maximum value of five and is similar to the siderophyllite end-member: $K(Fe_2Al)(Al_2Si_2O_{10}(OH)_2$.

Oxide minerals

Two kinds of daughter minerals produced iron X-rays; one was tabular, suggesting hematite, the other was octahedral, which is typical of magnetite. In polished thin-sections both red flakes and black, equant, magnetic crystals were observed, indicating that both oxides may be present. However, as discussed by Zolensky and Bodnar (1982), caution should be exercised in the interpretation of iron oxide mineralogy. They report the presence of martite (hematite after octahedral magnetite) in fluid inclusions from Copper Creek, Arizona.

Conclusions

1. The usefulness of scanning electron microscopy and energy dispersive analysis for the identification of daughter minerals is greatly enhanced by the application of standard data reduction procedures. Despite the very small size and irregular disposition of the surfaces of the daughter minerals, the analyses are sufficiently reproducible and accurate to allow identification of many minerals. Stoichiometry is usually within ten percent of the expected value.

2. The daughter minerals identified were halite, sylvite, calcium sulfate (anhydrite?), chalcopyrite, potassium feldspar, and two different micas—an iron-rich muscovite (or illite?) and an iron-rich trioctahedral mica similar to siderophyllite. The hydrothermal vein assemblage associated with the quartz for this study was biotite, potassium feldspar, and quartz; thus the daughter mineral assemblage parallels the vein-filling and alteration assemblage. Significant differences between the two assemblages are the apparent paucity of magnesium in the daughter minerals compared to the alteration minerals and the presence of chalcopyrite in fluid inclusions.

Acknowledgments

References

Chryssoulis, S. and Wilkinson, N. (1983) High silver content of fluid inclusions in quartz from Guadalcazar Granite, San Luis Potosi, Mexico: A contribution to ore genesis theory. Economic Geology, 78, 302–318.

Kelly, W. C., and Burgio, P. A. (1983) Cryogenic scanning electron microscopy of fluid inclusions in ore and gangue minerals. Economic Geology, 78, 1262–1267.

Kulikov, I. V., Devyatov, V. Y., and Gromov, A. V. (1982) On a new natural compound: calcium fluoride chloride. (in Russian) Izvestiya Vysshikh Uchebnykh Zavednii (Geologiya i Razvedka), 25, 120–122.

LeBel, Laurent (1976) Note preliminaire sur la mineralogie des phases solides contenues dans les inclusions des phenocristaux de quartz du porphyre cuprifere de Cerro Verde/Santa Rosa, Perou meridional. Bulletin Societe Vaud. Science Naturale, 73, 201–208.

Metzger, F. W., Kelly, W. C., Nesbitt, B. E., and Essene, E. J. (1977) Scanning electron microscopy of daughter minerals in fluid inclusions. Economic Geology, 72, 141–152.

Reynolds, T. J. (1980) Variations in hydrothermal fluid characteristics through time at the Santa Rita porphyry copper deposit, New Mexico. M.S. thesis. University of Arizona, Tucson.

Roedder, E. (1972) Composition of fluid inclusions. In M. Fleischer, Ed., Data of Geochemistry, 6th edition, U.S. Geological Survey Professional Paper 440JJ.

Roedder, E. (1979) Fluid inclusions as samples of ore fluids. In H. L. Barnes, Ed., Geochemistry of Hydrothermal Ore Deposits, 2nd edition, p. 684–737. John Wiley and Sons, New York.

Rosasco, G. J. and Roedder, E. (1979) Application of a new microprobe spectrometer to non-destructive analysis of sulfate and other ions in individual phases in fluid inclusions in minerals. Geochimica and Cosmochimica Acta, 43, 1907–1916.

Sawkins, F. J., and Scherkenbach, D. A. (1981) High copper content of fluid inclusions in quartz from northern Sonora: Implications for ore genesis theory. Geology, 9, 37–40.

Wilson, J. W. J., Kesler, S. E., Cloke, P. L., and Kelly, W. C. (1980) Fluid inclusion geochemistry of the Granisle and Bell porphyry copper deposits, British Columbia. Economic Geology, 75, 45–61.

Zolensky, M. E., and Bodnar, R. J. (1982) Identification of fluid inclusion daughter minerals using Gandolfi X-ray techniques. American Mineralogist, 67, 134–141.